Title: Matrix metalloproteinase-3 is a possible mediator of neurodevelopmental impairment due to polyI:C-induced innate immune activation of astrocytes

Authors: Shinnosuke Yamada[*], Taku Nagai[*], Tsuyoshi Nakai, Daisuke Ibi, Akira Nakajima, Kiyofumi Yamada[#]

Affiliation: Department of Neuropsychopharmacology and Hospital Pharmacy, Nagoya University Graduate School of Medicine, Nagoya 466-8560, Japan

*Contributed equally to this work

[#]**Corresponding author:** Kiyofumi Yamada, Ph.D.

Department of Neuropsychopharmacology and Hospital Pharmacy, Nagoya University Graduate School of Medicine, 65 Tsuruma-cho, Showa-ku, Nagoya 466-8560, Japan

Tel.: +81-52-744-2674, Fax: +81-52-744-2979,

E-mail: kyamada@med.nagoya-u.ac.jp

Keywords: astrocyte; neuron; polyI:C; viral infection; immune response; neuron–glia interactions; secretome; cytokine; Mmp3; schizophrenia

Abstract

Increasing epidemiological evidence indicates that prenatal infection and childhood central nervous system infection with various viral pathogens enhance the risk for several neuropsychiatric disorders. Polyriboinosinic-polyribocytidilic acid (polyI:C) is known to induce strong innate immune responses that mimic immune activation by viral infections. Our previous findings suggested that activation of the innate immune system in astrocytes results in impairments of neurite outgrowth and spine formation, which lead to behavioral abnormalities in adulthood. To identify candidates of astrocyte-derived humoral factors that affect neuronal development, we analyzed astrocyte-conditioned medium (ACM) from murine astrocyte cultures treated with polyI:C (polyI:C-ACM) by two-dimensional fluorescence difference gel electrophoresis (2D-DIGE). Through a quantitative proteomic screen, we found that 13 protein spots were differentially expressed compared with ACM from vehicle-treated astrocytes (control-ACM), and characterized one of the candidates, matrix metalloproteinase-3 (Mmp3). PolyI:C treatment significantly increased the expression levels of Mmp3 mRNA and protein in astrocytes, but not microglia. PolyI:C-ACM was associated with significantly higher Mmp3 protein level and enzyme activity than control-ACM. The addition of recombinant Mmp3 into culture media impaired dendritic elongation of primary cultured hippocampal neurons, while the deleterious effect of polyI:C-ACM on neurite elongation was attenuated by knockdown of Mmp3 in astrocytes. These results suggest that Mmp3 is a possible mediator of polyI:C-ACM-induced neurodevelopmental impairment.

1. Introduction

Abnormalities in early brain development contribute to the etiology of many neurological disorders in later life (Grabrucker, 2012; Schmidt-Kastner et al., 2012; van Dongen and Boomsma, 2013). Recent advances in genome analysis indicate that large numbers of common variants shape an individual's disease risk, including that for major mental illnesses (Cross-Disorder Group of the Psychiatric Genomics et al., 2013; Ripke et al., 2013; Walters et al., 2013), although the biological mechanisms by which environmental components affect brain development are poorly understood. Environmental insults include maternal stress, nutritional deficiencies, perinatal infections, season of birth and obstetric complications (Brown, 2011; Dean and Murray, 2005). Several lines of epidemiological evidence suggest that prenatal infection and childhood central nervous system (CNS) infection with various viral pathogens enhance the risk for several neuropsychiatric disorders including schizophrenia (Brown et al., 2004; Khandaker et al., 2012; O'Callaghan et al., 1994), autism (Grabrucker, 2012) and mental retardation (Revello and Gerna, 2004). These findings indicate the possible interference in normal brain development by abnormal immune responses.

On the basis of the epidemiological evidence, some animal models for the effects of viral infection on brain development have been established (Meyer and Feldon, 2010; Nagai et al., 2011; Nawa and Takei, 2006). One of these is maternal exposure to polyriboinosinic-polyribocytidylic acid (polyI:C). PolyI:C is a synthetic analogue of double-stranded RNA that is recognized by the pattern recognition receptor, toll-like receptor (TLR) 3, and then evokes an antiviral-like inflammatory response (Alexopoulou et al., 2001). This response includes a profound increase in the production of many pro-inflammatory cytokines including interleukin (IL)-1β, IL-6, tumor necrosis factor (TNF)-α and type I interferons (IFN-α and IFN-β) (Fortier et al.,

2004; Takeuchi and Akira, 2007). Adult offspring that received prenatal treatment with polyI:C displayed significant behavioral abnormalities in sociability, emotion, sensorimotor gating, cognition and working memory (Meyer et al., 2005; Ozawa et al., 2006; Shi et al., 2003; Smith et al., 2007). We also previously demonstrated that neonatal treatment of mice with polyI:C induced impairment in sociability, emotion, sensorimotor gating and cognition in adulthood (Ibi et al., 2009). The induction of interferon-induced transmembrane 3 (Ifitm3) in astrocytes has a crucial role in polyI:C-induced neurodevelopmental abnormalities including impairments of dendrite elongation and spine formation, which lead to behavioral impairments in adulthood (Ibi et al., 2013). Thus, it is proposed that Ifitm3 might be a novel drug target for the treatment of schizophrenia (Horvath and Mirnics, 2013).

Glial cells have been widely recognized as essential regulators of neuronal development including neuronal migration, axon and dendrite growth, formation of synapses and synaptic plasticity (Hamilton and Attwell, 2010; Volterra and Meldolesi, 2005), although they are classically thought to provide structural and metabolic support for neurons. Astrocytes also play a critical role in regulating CNS immune response by responding to inflammatory mediators and producing additional cytokines and chemokines (Dong and Benveniste, 2001). Most of the functions of astrocytes are mediated by the release of humoral factors through a close interaction with neurons. Our previous results suggested that activation of the innate immune system in astrocytes alters the components of the extracellular environment including downregulation of neurotrophic factors and upregulation of neurodegenerative ones (Ibi et al., 2013). However, the mechanism by which innate immune activation of astrocytes affects neuronal development remains to be determined. In this study, to explore the alteration in proteins secreted from murine astrocytes after polyI:C stimulation, astrocyte-conditioned medium (ACM) was analyzed by 2-dimensional

fluorescence difference gel electrophoresis (2D-DIGE). Here, we identified matrix metalloproteinase-3 (Mmp3, also known as stromelysin-1) as a potential mediator of polyI:C-ACM-induced neurodevelopmental impairment.

2. Materials and Methods

2.1. Animals

Institute of Cancer Research (ICR) and C57BL/6J mice were purchased from Japan SLC Inc. (Hamamatsu, Japan). ICR mice (closed colony) were used for 2D-DIGE analysis to detect general responses to the polyI:C treatment for astrocytes, while C57BL/6J mice (inbred strain) were used for keeping uniformity of the experiments. The animals had free access to food (CE-2, Clea Japan, Tokyo, Japan) and water and were kept under controlled conditions (23±1°C) with a constant light-dark cycle (light 9:00-21:00). All animals were handled in accordance with the guidelines established by the Institutional Animal Care and Use Committee of Nagoya University, the Guiding Principles for the Care and Use of Laboratory Animals approved by the Japanese Pharmacological Society and the National Institutes of Health Guide for the Care and Use of Laboratory Animals.

2.2. Astrocyte culture and ACM preparation

Secondary astrocyte cultures were prepared as previously described (Ibi et al., 2013). Briefly, cortices and hippocampi of neonatal ICR (for 2D-DIGE) or C57BL/6J mice at postnatal day (PD) 1-2 were mechanically dissociated and digested for 15 min at 37°C with 0.3% dispase (Roche Diagnostics GmbH, Mannheim, Germany) and 0.4% DNase (Roche Diagnostics GmbH). The cells were suspended in culture medium [Dulbecco's Modified Eagle's Medium (DMEM, Sigma-Aldrich, St. Louis, MO) containing 10% fetal bovine serum (FBS, Gibco-BRL, Gaithersburg, MD)] and filtered through a 40-μm nylon cell strainer (Falcon-Becton Dickinson, Le Pont de Claix, France). The cell suspension was cultured in a T150 flask at a density of six neonate brains per flask at 37°C with 5% CO_2. The confluent primary astrocyte cultures were purified by shaking, and plated into 6- or 24-well plates and grown to

confluence in all experiments. Under these conditions, more than 95% of cells were glial fibrillary acidic protein (GFAP)-positive (a marker for astrocytes) and negative for tau/MAP2 and CD11b (neuronal and microglial markers, respectively). Culture medium was replaced with Neurobasal Medium (Invitrogen, Eugene, OR) supplemented with B-27 (Invitrogen) and 1 mM glutamine (Sigma-Aldrich) 6 days before the treatment with polyI:C (Sigma-Aldrich). This medium was renewed 3 days and 24 h before the treatment with polyI:C. For 2D-PAGE and western blotting, B-27 was excluded from the last medium. Astrocytes were treated with PBS (control) or polyI:C (10 μg/mL) and conditioned medium was collected 24 h after the polyI:C treatment. For the time course analysis, conditioned medium was collected 6 h and 12 h after the polyI:C treatment. These conditioned media were centrifuged at 1000 × g for 10 min at 4°C and the supernatants were used as ACM.

2.3. Microglia culture and microglia-conditioned medium (MCM) preparation

Two weeks after seeding of primary astrocyte cultures, microglia were separated from the underlying astrocytic monolayer by shaking for 3 h at 150 rpm. The supernatants including floating microglia were centrifuged at 1,000 rpm for 10 min and pellet was resuspended in fresh culture medium. Microglia were plated at 1 × 10^6 cells/well in a 6-well plate and culture medium was replaced with Neurobasal Medium supplemented with 1 mM glutamine 1 h after plating. The microglial cultures were >98% pure assessed by immunocytochemistry with an anti-Iba1 antibody (Wako, Osaka, Japan) in combination with an anti-GFAP antibody (Sigma-Aldrich) as markers for microglia and astrocytes, respectively. PBS (control) or polyI:C (10 μg/mL) were treated 24h after the medium change and conditioned media were collected 24 h after the polyI:C treatment. The conditioned media were centrifuged at 1000 × g for 10 min at 4°C and the supernatants were used as MCM.

2.4. Primary cultured neurons and ACM treatment

Primary cultured hippocampal neurons were prepared from C57BL/6J mice on gestational day 15-16, as described previously (Ibi et al., 2013). Briefly, embryo hippocampi were trypsinized (with 0.25% trypsin and 0.01% DNase) followed by trituration and seeded on coverslips precoated with 0.1 mg/ml poly-D-lysine at a low density (1.0×10^4 cells/well in a 24-well plate). Cells were cultured in Neurobasal Medium with B-27 and 1 mM glutamine. The medium was replaced with polyI:C-ACM or control-ACM and supplemented with 0.75 μM cytosine β-D-arabinofuranoside (Ara-C, Sigma-Aldrich) on DIV2. In the functional studies, pro-form of recombinant mouse (rm) Mmp3 (R&D Systems) was added to control-ACM at final concentrations of 10 nM and 100 nM on DIV2. The effects of ACM on dendritic elongation were assayed on DIV7. More than 99% pure neurons, as demonstrated by anti-tau or anti-MAP2 immunostaining, were obtained from this preparation.

2.5. Knockdown assay

siRNA transfection was performed at 6 h before the last medium change. Astrocytes were transfected with Stealth siRNA for Mmp3 (#1 sense: UCUCUCAAGAUGAUGUAGAUGGUAU, #1 antisense: AUACCAUCUACAUCAUCUUGAGAGA; #2 sense: UCAGUGGAUCUUCGCAGUUGGAAUU, #2 antisense: AAUUCCAACUGCGAAGAUCCACUGA) or Stealth RNAi siRNA negative control (control siRNA) using Lipofectamine RNAiMAX transfection reagent (all from Invitrogen).

2.6. 2D-DIGE analysis for polyI:C-ACM

PolyI:C-ACM and control-ACM were concentrated by ultrafiltration of ACM using Vivaspin 15R Hydrosart 5,000 MWCO (Sartorius Stedim Biotech GmbH, Göttingen, Germany). Proteins were precipitated with methanol/acetone and reconstituted in resuspension buffer [30 nM Tris–HCl (pH 8.5), 4% CHAPS, 7 M urea, 2 M thiourea]. Protein concentration was determined using a protein assay kit (Bio-Rad Laboratories, Hercules, CA) and adjusted to 3 mg/ml using resuspension buffer. For the fluorescent labeling of proteins, CyDye DIGE Fluor, minimal labeling kit (GE Healthcare, Chalfont St. Giles, Buckinghamshire, UK) was used according to the manufacturer's protocol. In brief, an equal amount of protein (36 μg) from each ACM was individually labeled using 240 pmol of either Cy3 or Cy5. To exclude any labeling bias by the different dyes, a sample of each group was reciprocally labeled with Cy3 or Cy5. An equal pool of all samples was prepared as an internal standard (IS) and IS protein was labeled with Cy2. IS was included for spot normalization to allow comparison across all gels. Each protein was incubated with dyes for 30 min on ice and the labeling reaction was quenched using 0.6 μl of 10 mM lysine for 10 min. Labeled protein samples were diluted with an equal volume of sample buffer [40 mM dithiothreitol (DTT), 4% CHAPS, 7 M urea, 2 M thiourea and 1% pharmalyte (pH 3-10)]. Different kinds of fluorescent-labeled protein from polyI:C-ACM, control-ACM and IS were mixed before loading on the gel.

Sample volume was adjusted to 450 μl with rehydration buffer (20 mM DTT, 4% CHAPS, 7 M urea, 2 M thiourea, 0.5% pharmalyte pH 3-10 and 0.001% bromophenol blue) and samples were loaded on a 24 cm Immobiline Drystrip, pH3-10 NL gel (GE Healthcare). After rehydration of the drystrip gels for 12 h at 20°C, isoelectric focusing (IEF) was performed as follows: less than 50 μA per drystrip gel at 20°C, 30 V/2 h, 100 V/1 h, 200 V/5 min, gradient to 8,000 V/8.5 h, constant 8,000 V until

reaching 60,000 Vh. After reduction and alkylation of drystrip gels with 1% DTT (Wako) and 2.5% iodoacetamide (Sigma-Aldrich) in SDS equilibration buffer [50mM Tris-HCl (pH 8.8), 6 M urea, 30% glycerol, 2% SDS], the second-dimension separation was carried out on a 10% acrylamide gel. The gels were scanned at 100 mm resolution using a Typhoon Trio laser scanner (GE Healthcare).

The scanned images were analyzed using PDQuest Advanced Version 8.0 software (Bio-Rad). Protein spots were automatically detected and visually modified for undetected or incorrectly detected spots. All protein spots detected in each image were linked among all the analyzed images. Each Cy3- or Cy5-labeled protein spot intensity was normalized by the spot volume of the corresponding protein spot in the IS image and total spot intensity was adjusted for all the images. The ratio of individual spot intensity was also determined by each spot's intensity divided by the total spot intensity of each image.

2.7. In-gel digestion and nano-LC-MS/MS for protein identification

A preparative gel was prepared by 2D-PAGE using control-ACM proteins without fluorescent labeling. The gel was visualized by silver staining and spots of interest were excised from it. The gel pieces were digested with 20 ng/μl trypsin (sequencing grade, Promega Benelux, Leiden, The Netherlands), and the resulting peptides were analyzed using a paradigm MS4 HPLC system (Michrom BioResources, Auburn, CA) equipped with an LCQ advantage mass spectrometer (Thermo Fisher Scientific, San Jose, CA). Each sample of peptides dried after in-gel digestion was reconstituted in reverse-phase buffer and transferred to a paradigm MS4 HPLC system equipped with a magic C18AQ column of 0.1 mm in diameter and 50 mm in length (Michrom BioResources). Reversed-phase chromatography was performed with a linear gradient (0 min, 5% solvent B; 45 min, 100% solvent B) of

solvent A (2% acetonitrile in 0.1% formic acid) and solvent B (90% acetonitrile in 0.1% formic acid) at an estimated flow rate of 1 μl/min. Ionization was performed using an ADVANCE CaptiveSpray Source (Michrom BioResources) with a capillary voltage of 1.7 kV and temperature of 150°C. A precursor ion scan was carried out using a 400–2000 mass to charge ratio (m/z) prior to MS/MS analysis. Multiple MS/MS spectra were used for searching the Swiss-Prot protein database using a MASCOT program (Matrix Science, Boston, MA) for the MS/MS ion search with 2.0 D mass tolerance.

2.8. Western blotting

ACM and MCM were concentrated using Vivaspin 2 Hydrosart 5,000 MWCO (Sartorius Stedim Biotech GmbH). After removing the conditioned medium, the remaining cells were washed with ice-cold PBS and collected in lysis buffer [20 mM Tris-HCl (pH 7.4), 150 mM NaCl, 50 mM NaF, 2 mM EDTA, 1% Triton X-100, 1 mM sodium orthovanadate, 0.1% SDS, 1% sodium deoxycholate and protease inhibitor cocktail (Sigma-Aldrich)]. Protein lysates were centrifuged at 15,000 × g for 20 min. ACM or cell lysates were denatured in Laemmli sample buffer containing 20% β-mercaptoethanol at 95°C for 5 min. An equal amount of protein for each sample was separated by 10% SDS-PAGE and transferred to a polyvinylidene fluoride (PVDF) membrane (Millipore). The membrane was blocked with detector block solution (KPL, Gaithersburg, MD). After blocking, the membrane was incubated with rabbit anti-Mmp3 antibody (Abcam, Cambridge, UK) or goat anti-actin antibody (Santa Cruz Biotechnology, Santa Cruz, CA) at 4°C overnight. After incubation with an appropriate horseradish peroxidase-conjugated secondary antibody [anti-rabbit (KPL) or anti-goat antibody (R&D Systems, Minneapolis, MN)] for 2 h, the membrane was incubated with ECL prime western blotting detection reagents (GE Healthcare)

and protein bands were detected using a luminescent image analyzer (Atto, Tokyo, Japan).

2.9. Total RNA isolation and real-time RT-PCR

After removing the conditioned medium, total RNA of astrocytes and microglia were prepared using RNeasy Mini Kit (Qiagen, Hilden, Germany) and converted into complementary DNA (cDNA) using the SuperScript III First-Strand Synthesis Kit (Invitrogen). Quantitative real-time PCR was performed on a 7300 Real-Time PCR System (Applied Biosystems, Foster City, CA) using Power SYBR Green Master Mix (Applied Biosystems) according to the manufacturer's protocol. The primers used were as follows: forward, TCCCGTTTCCATCTCTCTCAA and reverse, GGATGCTGTGGGAGTTCCATA for Mmp3; forward, TCATTTTCGTTATCACACACCATTT and reverse, TGAACTGCGTGATGTACCTTGAA for Tlr3; and forward, CGATGCCCTGAGGCTCTTT and reverse, TGGATGCCACAGGATTCCA for β-actin used as an internal control. Real-time PCR reactions were conducted as follows: initial 2 min incubation at 50°C and 10 min incubation at 95°C, followed by 40 reaction cycles of 95°C for 15 sec and 60°C for 1 min. Fluorescent signals were monitored at the extension step of 60°C in each cycle. For each sample test, each PCR reaction had 2 replicates and relative gene expression differences were quantified using the comparative Ct method (ΔΔCt).

2.10. Zymographic analysis

Non-concentrated ACM was mixed with Laemmli sample buffer without β-mercaptoethanol and incubated for 10 min at room temperature. Caseinolytic activities of Mmp3 were determined by zymography using 12% polyacrylamide gels

containing 0.1% casein (Sigma-Aldrich). The gels were incubated in denaturing buffer [50 mM Tris-HCl (pH 7.4), 5 mM $CaCl_2$, 5 μM $ZnCl_2$ and 2.5% Triton X-100] for 20 min three times to remove SDS and then incubated in developing buffer [50 mM Tris-HCl (pH 7.4), 5 mM $CaCl_2$, 5 μM $ZnCl_2$ and 0.01% NaN_3] for 48 h at 37°C. After incubation, gels were stained in 0.5% Coomassie blue R-250 for 1 h and destained with 40% methanol and 10% acetic acid. Gels were imaged using a densitometer (Atto). Proteolytic activities that appeared as clear bands against a dark background of stained casein were analyzed using ImageJ software (from NIH, available at http://rsb.info.nih.gov/ij/). Recombinant mouse Mmp3 (R&D Systems) was used as a positive control and determination of Mmp3 concentration in polyI:C-ACM was carried out by applying the absolute calibration curve method.

2.11. Immunocytochemistry

Cells were fixed in 4% paraformaldehyde in 0.1 M phosphate buffer for 20 min and then permeabilized with 0.1% Triton X-100 for 10 min. After incubation in blocking solution (1% goat and 1% donkey serum in PBS) for 30 min, mouse anti-tau (1:500, Santa Cruz Biotechnology) and rabbit anti-MAP2 (1:1000, Millipore) antibodies diluted in blocking solution were applied to the cells. After overnight incubation with primary antibodies at 4°C, the cells were treated with goat anti-mouse Alexa Fluor (AF) 488 and anti-rabbit AF568 antibodies (1:1,000; Invitrogen) for 2 h at room temperature. The cells were mounted in fluorescence mounting medium (Dako, Glostrup, Denmark) and photographed under a fluorescence microscope (Zeiss, Jena, Germany) using AxioCam MRc5 (Zeiss).

2.12. Neurite elongation assay

Dendritic elongation of cultured hippocampal neurons was analyzed in

accordance with a previous study (Ibi et al., 2013). Axons were identified by double immunostaining in terms of tau-positive (axonal marker) and MAP2-negative (dendritic marker) and only MAP2-positive neurites being defined as dendrites. Neurons that clearly had tau- or MAP2-positive neurites were selected randomly by an expert researcher who was blinded to the experimental groups. Dendrites were traced automatically with the same configuration using Neurolucida software (MicroBrightField, Williston, VT) and total dendritic length in a single neuron was calculated using Neuroexplorer (MicroBrightField). This assay was carried out 3 independent experiments.

2.13. Statistical analysis

Data are shown as the mean±SE. Differences between two groups were analyzed by two-tailed Student's t-test. One-way and two-way analysis of variance (ANOVA) followed by Bonferroni post hoc test was applied for differences in three or more groups.

3. Results

3.1. Differential expression of extracellular proteins in polyI:C-ACM

Figure 1A shows a representative merged 2D-DIGE image of polyI:C-ACM and control-ACM. The proteins in polyI:C-ACM are shown in red and the control-ACM in green, indicating that green spots represent down-regulated proteins, while red spots correspond to proteins up-regulated in polyI:C-ACM. Overall, 422 unique protein spots could be detected in all images of this experiment. Statistical analysis revealed that the signal intensities of 13 spots were significantly altered in polyI:C-ACM, among which 2 spot intensities were increased while 11 were decreased (Fig. 1B and Table 1). The proteins were successfully identified from all spots analyzed with a high MASCOT score and no gross variations between the experimental molecular weight (MW)/isoelectric point (pI) and theoretical MW/pI of the proteins (Table 2).

3.2. Upregulation of Mmp3 in polyI:C-ACM

Proteomic analysis revealed remarkable changes in the extracellular levels of several proteins from polyI:C-treated astrocytes. Among these proteins, matrix metalloproteinase-3 (Mmp3) was thought to be one of the major components in polyI:C-ACM because the intensity of spot #7 constituted 3.32 ± 0.44% (n = 5) of the total spot intensity in it. Furthermore, a previous study reported the association of polymorphism of *MMP3* with schizophrenia (Kucukali et al., 2009), so we focused on Mmp3 in subsequent experiments. First of all, we examined the temporal changes in Mmp3 mRNA and protein levels in astrocytes after polyI:C treatment. Two-way ANOVA revealed significant effects of polyI:C on Mmp3 mRNA (polyI:C treatment: $F(1,12) = 528.8$, $p<0.01$; time: $F(2,12) = 21.24$, $p<0.01$; interaction: $F(2,12) = 38.07$, $p<0.01$, Fig. 2B) and protein levels (polyI:C treatment: $F(1,48) = 71.07$, $p<0.01$; time:

F(2,48) = 2.43, p=0.10; interactiont: F(2,48) = 2.06, p=0.14, Fig. 2A, C). The mRNA and protein levels of Mmp3 in the cell lysate of astrocytes were significantly increased at 6 h, 12 h and 24 h after the polyI:C treatment ($p<0.01$, Fig. 2A-C). PolyI:C had effects on protein level of Mmp3 in ACM (polyI:C treatment: F(1,30) = 102.0, $p<0.01$; time: F(2,30) = 63.55, $p<0.01$; interaction: F(2,30) = 46.56, $p<0.01$, Fig. 2A, D) and a significant increase in Mmp3 protein level in ACM was detected at 12 h and 24 h after the treatment ($p<0.01$, Fig. 2D). Protease activity of Mmp3 in ACM was analyzed by casein zymography. Caseinolytic activity of Mmp3 in polyI:C-ACM was significantly increased to approximately 20-fold that of control-ACM 24 h after the treatment ($p<0.05$, Fig. 2E). The concentration of Mmp3 in polyI:C-ACM was estimated to be 11.7 ± 1.2 nM (n = 4) by applying the absolute calibration curve method using various concentrations of rmMmp3 (0 to 20 nM).

3.3. Mmp3 expression in astrocyte and microglia

It is well known that TLR3 is a major receptor for polyI:C and we have previously reported that polyI:C treatment increases the Tlr3 expression in astrocytes (Ibi et al., 2013). In addition to astrocytes, microglia is a major immunocompetent cell in the CNS. Therefore, we explored the expression levels of Tlr3 and Mmp3 mRNA in microglia with or without polyI:C treatment. A two-way ANOVA revealed significant interactions between cell type and polyI:C treatment with respect to the Tlr3 mRNA (F(1,12) = 30.95, $p<0.01$, Fig. 3A) and Mmp3 mRNA levels (F(1,22) = 35.50, $p<0.01$, Fig. 3B). The basal mRNA levels of Tlr3 and Mmp3 in microglia were much lower than that in astrocytes. A multiple-comparison test with Bonferroni post-hoc tests indicated that polyI:C treatment induced the expression of Tlr3 and Mmp3 mRNA in astrocytes, but not in microglia ($p<0.01$, Fig 3A, 3B). Furthermore, Mmp3 protein level in MCM could not be detected with or without polyI:C treatment although Mmp3

protein level was significantly increased in polyI:C-ACM as compared to control-ACM ($p<0.01$, Fig. 3C).

3.4. Effect of Mmp3 on the dendritic elongation of primary cultured neurons

Our previous study demonstrated that polyI:C-ACM impairs the dendritic elongation of cultured hippocampal neurons (Ibi et al., 2013). To assess whether Mmp3 could mimic the effect of polyI:C-ACM on hippocampal neurons, dendritic elongation of primary cultured hippocampal neurons was measured after rmMmp3 treatment. The addition of rmMmp3 to the ACM on DIV2 resulted in a concentration-dependent decrease in dendritic elongation of primary cultured neurons on DIV7 ($F(2,108) = 34.88$, $p<0.01$, Fig. 4). The decrements of dendritic elongation induced by rmMmp3 were 21% and 52% compared with control-ACM at concentrations of 10 nM ($p<0.01$) and 100 nM ($p<0.01$), respectively (Fig. 4).

By applying an RNA interference method, we further examined whether Mmp3 mediates the impairment of dendritic elongation induced by polyI:C-ACM. Mmp3 mRNA and protein levels in control siRNA-transfected astrocytes were significantly increased after polyI:C treatment compared with the levels in control treatment (Fig. 5B: $F(3,12) = 146.91$, $p<0.01$, Fig. 5A, 5C: $F(3,12) = 5.98$, $p<0.05$). PolyI:C failed to induce Mmp3 mRNA and protein in astrocytes transfected with Mmp3 siRNA (Mmp3 siRNA #1 or #2) ($p<0.01$, Fig. 5B and $p<0.05$, Fig. 5C). Mmp3 protein level in polyI:C-ACM was also maintained at the control level when astrocytes were transfected with either Mmp3 siRNA #1 or #2 (Fig. 5A, 5D: $F(3,12) = 29.15$, $p<0.01$). Under such experimental conditions, polyI:C-ACM-induced impairment of dendritic elongation was significantly, but partially, attenuated ($F(3,174) = 95.23$, $p<0.01$, Fig. 5E). Equivalent ameliorating effects were observed in Mmp3 knockdown ACM (Mmp3 siRNA #1 and #2), with approximately 30% recovery compared with the

dendrite length in neurons cultured with control siRNA-treated polyI:C-ACM (Fig. 5E).

4. Discussion

Astrocytes play a significant role in neural function through the modulation of neurotransmitters or the release of gliotransmitters such as glutamate, ATP and D-serine (Hamilton and Attwell, 2010; Volterra and Meldolesi, 2005). In addition, the indispensable nature of the contribution of astrocytes to neural development, synaptic formation and maintenance of the blood-brain barrier has been demonstrated (He and Sun, 2007; Ullian et al., 2004; Wang and Bordey, 2008). Increasing research focused on astrocytes should discover humoral factors that are responsible for neuron-glia interactions. It has been reported that thousands of proteins are released from astrocytes in the presence of cholinergic agonist, proinflammatory cytokines, angiogenin, β-amyloid peptide 1-42 and lipopolysaccharide (LPS) (Delcourt et al., 2005; Keene et al., 2009; Lafon-Cazal et al., 2003; Lai et al., 2013; Moore et al., 2009; Skorupa et al., 2013). In the present study, we focused on alterations in the levels of proteins released from astrocytes after innate immune activation by treatment with polyI:C, as we have reported that polyI:C impairs the dendritic elongation of hippocampal neurons through astrocyte-derived humoral factors (Ibi et al., 2013). We detected 422 protein spots on 2D-DIGE images of ACM; 13 differentially expressed spots in polyI:C-ACM were subsequently identified.

We selected spot #7, representing Mmp3 as identified by LC/MS/MS, as a candidate molecule because of its high expression level in polyI:C-ACM, although the change of spot #1 was greater than that of spot #7. Moreover, a possible relationship between −1171 5A/6A polymorphism of *MMP3* and schizophrenia has been reported (Kucukali et al., 2009). This genetic association study revealed that the 5A/5A genotype and 5A allele distributions of *MMP3* are significantly common in patients with schizophrenia (Kucukali et al., 2009). Interestingly, the genetic variations of −1171 5A/6A are located on the promoter sequence of *MMP3* and in vitro

studies demonstrated that the 5A allele has higher promoter activity than the 6A allele (Ye et al., 1996). A recent study also suggested that the 5A/5A genotype is significantly increased in patients with Alzheimer's disease (Flex et al., 2013). Considering these previous findings, we first investigated the role of Mmp3 in neurodevelopmental impairment associated with polyI:C-induced innate immune activation of astrocytes. Functional analysis of other candidate proteins including spot #1 is in progress.

We first confirmed the time-dependent increases in Mmp3 mRNA and protein levels in polyI:C-treated astrocytes. The cellular mRNA and protein levels of Mmp3 were significantly increased 6 h after polyI:C treatment, while a significant increase in extracellular Mmp3 protein level was detected 12 h later. Furthermore, knockdown of Mmp3 prevented the polyI:C-induced increase of extracellular Mmp3. These results suggest that polyI:C treatment increases extracellular Mmp3 level in a transcription-dependent manner, although the molecular mechanism behind this in astrocytes remains to be determined. Since our previous study indicated that polyI:C treatment affected endocytosis in astrocytes (Ibi et al., 2013), the secretion and uptake of Mmp3 need to be determined.

Although TLR3 is a primary receptor for polyI:C and plays a fundamental role in the activation of innate immunity (Alexopoulou et al., 2001), the expression of Tlr3 in polyI:C-treated microglia is controversial. Some previous reports indicated upregulation of the level of TLR3 expression, but others showed that polyI:C had no effect (Olson and Miller, 2004; Town et al., 2006). Meanwhile, Mmp3 is highly expressed in astrocytes, but weakly in microglia (Ito et al., 2007). In the present study, basal Tlr3 and Mmp3 expression levels in microglia were much lower than those in astrocytes, and polyI:C treatment had no effect on the expression levels of Tlr3 and Mmp3 in microglia. These results indicate that astrocytes are the primary

source of Mmp3 under our experimental conditions.

Previous studies reported that the release of Mmp3 in ACM was significantly increased after treatment with a mixture of proinflammatory cytokines including IL-1β, IFN-γ and TNFα (Keene et al., 2009). Among these, IL-1β and TNFα were reported to increase the expression of Mmp3 in primary cultures of mouse brain astrocytes, but IFN-γ was not effective (Crocker et al., 2006; Witek-Zawada and Koj, 2003). We also reported the changes in expression levels of cytokines 24 h after polyI:C treatment in astrocytes and that a series of proinflammatory cytokines including IL-1β and TNFα were up-regulated in polyI:C-treated astrocytes (Ibi et al., 2013). Therefore, it is possible that polyI:C treatment induces the production and release of Mmp3 through proinflammatory cytokine upregulation.

In this study, astrocyte culture was prepared from cortices and hippocampi, but the properties of astrocytes might differ between two regions (Cordero-Llana et al., 2011). We confirmed the Mmp3 expression in ACM and astrocytes prepared from hippocampi and cortices separately. There was no difference in the basal expression of Mmp3 or in the response to polyI:C treatment between astrocyte cultures prepared from two brain regions (data not shown). It is likely that the dynamic changes in Mmp3 in response to polyI:C treatment are comparable between cortical and hippocampal astrocytes.

We further examined the biological activity of Mmp3 on the dendritic elongation of cultured hippocampal neurons. Mmp3 suppressed the dendritic elongation in a concentration-dependent manner and 10 nM rmMmp3, a concentration comparable to that estimated to exist in polyI:C-ACM, significantly reduced the total dendritic length of hippocampal neurons. In contrast, knockdown of Mmp3 in astrocytes partially but significantly attenuated the toxic potential of polyI:C on neurite development. These results indicate that Mmp3 is one of the factors responsible for

polyI:C-ACM-induced impairments of neuronal development and that factors other than Mmp3 are also involved.

Recently, Kim *et al.* (2010b) have reported a role of Mmp3 in the development of dopaminergic neurons in Mmp3 knockout (KO) mice. Mesencephalic neurons from Mmp3 KO showed an increase in the number of tyrosine hydroxylase (TH)-immunopositive neurites compared with those of the wild type (Kim et al., 2010b). Mmp3 also participates in apoptotic signaling and α-synuclein aggregation through the activation of intracellular Mmp3 in response to cellular stresses (Choi et al., 2011; Kim et al., 2010a; Levin et al., 2009). Furthermore, Mmp3 released from apoptotic cells triggers microglial activation, which further contributes to the neurodegenerative process (Kim et al., 2007). In our study, no apparent cell death after treatment with Mmp3 or microglial interaction for neuronal development was observed, so our results suggest that an excess amount of extracellular Mmp3 that was released by astrocytes after polyI:C treatment might have led to the disruption of dendritic elongation. Because we previously demonstrated that neonatal polyI:C treatment induces behavioral impairment in adulthood (Ibi et al., 2009), Mmp3 KO mice may be useful to confirm the role of Mmp3 in higher brain function *in vivo*.

Mmp3 degrades a variety of substrates, including extracellular matrix (ECM) and non-ECM proteins, and activates other Mmp subtypes (Chakraborti et al., 2003; Ethell and Ethell, 2007). For example, Mmp3 affects the cytoskeletal structure of neurons by regulating the activity of cell adhesion molecules such as integrins and N-syndecan (syndecan-3) (Asundi et al., 2003; Mercapide et al., 2003; Noe et al., 2001; Schulze-Tanzil et al., 2001). Hence, we need to study whether substrates for Mmp3 are involved in the impairment of neurite elongation. Further analyses are needed to elucidate the relationship between Mmp3 and Ifitm3 and the function of other proteins identified in this study for neuronal maturation. These analyses may

provide new insights into the effect of perinatal viral infections on brain development

A limitation of this study is that astrocytes were directly treated with polyI:C to explore the alterations of proteins secreted from murine astrocytes after innate immune activation. It should be noted that polyI:C is thought not to permeate the blood-brain barrier (BBB) or placenta under healthy conditions. Our findings in this study, therefore, might be regarded as an *in vitro* model of central viral infections and the consequent neurodevelopmental impairment (Pletnikov et al., 1999; Rubin et al., 1999). Previous reports, however, indicated that cytotoxic and proinflammatory substances could pass from the circulation into the brain after peripheral inflammatory stimulation when BBB permeability was increased in the fetal brain after exposure to endotoxin (Yan et al., 2004). In either case, much attention should be paid when interpreting our findings that Mmp3 is a possible mediator of neurodevelopmental impairment due to polyI:C-induced innate immune activation of astrocytes.

Conflict of interest statement

All authors declare that there are no conflicts of interest.

Acknowledgments

We thank the Division for Research of Laboratory Animals, Center for Research of Laboratory Animals and Medical Research Engineering, Nagoya University, for animal care and use (Yasutaka Ohya and Kumiko Yano), as well as LC-MS/MS analysis (Kentaro Taki). This work was supported by the following funding sources: JSPS KAKENHI (25003699) from JST, Exploratory Research from JSPS, “Integrated Research on Neuropsychiatric Disorders” and “Bioinformatics for Brain Sciences” carried out under the SRPBS from MEXT, CREST, Grants-in-Aid for Scientific Research (24111518, 25116515, 25460093) from MEXT, Health Labour Sciences

Research Grant (H25-Iyaku-Ippan-020) from MHLW, Intramural Research Grant (24-12) for Neurological and Psychiatric Disorders of NCNP, Grants for Project Research (Development of Fundamental Technology for Analysis and Evaluation of Functional Agricultural Products and Functional Foods) from the MAFF and an SRF Grant for Biomedical Research.

References

Alexopoulou, L., Holt, A.C., Medzhitov, R., Flavell, R.A., 2001. Recognition of double-stranded RNA and activation of NF-kappaB by Toll-like receptor 3. Nature 413, 732-738.

Asundi, V.K., Erdman, R., Stahl, R.C., Carey, D.J., 2003. Matrix metalloproteinase-dependent shedding of syndecan-3, a transmembrane heparan sulfate proteoglycan, in Schwann cells. J Neurosci Res 73, 593-602.

Brown, A.S., 2011. The environment and susceptibility to schizophrenia. Prog Neurobiol 93, 23-58.

Brown, A.S., Begg, M.D., Gravenstein, S., Schaefer, C.A., Wyatt, R.J., Bresnahan, M., Babulas, V.P., Susser, E.S., 2004. Serologic evidence of prenatal influenza in the etiology of schizophrenia. Arch Gen Psychiatry 61, 774-780.

Chakraborti, S., Mandal, M., Das, S., Mandal, A., Chakraborti, T., 2003. Regulation of matrix metalloproteinases: an overview. Mol Cell Biochem 253, 269-285.

Choi, D.H., Kim, Y.J., Kim, Y.G., Joh, T.H., Beal, M.F., Kim, Y.S., 2011. Role of matrix metalloproteinase 3-mediated alpha-synuclein cleavage in dopaminergic cell death. J Biol Chem 286, 14168-14177.

Cordero-Llana, O., Scott, S.A., Maslen, S.L., Anderson, J.M., Boyle, J., Chowhdury, R.R., Tyers, P., Barker, R.A., Kelly, C.M., Rosser, A.E., Stephens, E., Chandran, S., Caldwell, M.A., 2011. Clusterin secreted by astrocytes enhances neuronal differentiation from human neural precursor cells. Cell Death Differ 18, 907-913.

Crocker, S.J., Milner, R., Pham-Mitchell, N., Campbell, I.L., 2006. Cell and agonist-specific regulation of genes for matrix metalloproteinases and their tissue inhibitors by primary glial cells. J Neurochem 98, 812-823.

Cross-Disorder Group of the Psychiatric Genomics, C., Smoller, J.W., Craddock, N., Kendler, K., Lee, P.H., Neale, B.M., Nurnberger, J.I., Ripke, S., Santangelo, S.,

Sullivan, P.F., 2013. Identification of risk loci with shared effects on five major psychiatric disorders: a genome-wide analysis. Lancet 381, 1371-1379.

Dean, K., Murray, R.M., 2005. Environmental risk factors for psychosis. Dialogues Clin Neurosci 7, 69-80.

Delcourt, N., Jouin, P., Poncet, J., Demey, E., Mauger, E., Bockaert, J., Marin, P., Galeotti, N., 2005. Difference in mass analysis using labeled lysines (DIMAL-K): a new, efficient proteomic quantification method applied to the analysis of astrocytic secretomes. Mol Cell Proteomics 4, 1085-1094.

Dong, Y., Benveniste, E.N., 2001. Immune function of astrocytes. Glia 36, 180-190.

Ethell, I.M., Ethell, D.W., 2007. Matrix metalloproteinases in brain development and remodeling: synaptic functions and targets. J Neurosci Res 85, 2813-2823.

Flex, A., Giovannini, S., Biscetti, F., Liperoti, R., Spalletta, G., Straface, G., Landi, F., Angelini, F., Caltagirone, C., Ghirlanda, G., Bernabei, R., 2013. Effect of Proinflammatory Gene Polymorphisms on the Risk of Alzheimer's Disease. Neurodegener Dis, doi:10.1159/000353395.

Fortier, M.E., Kent, S., Ashdown, H., Poole, S., Boksa, P., Luheshi, G.N., 2004. The viral mimic, polyinosinic:polycytidylic acid, induces fever in rats via an interleukin-1-dependent mechanism. Am J Physiol Regul Integr Comp Physiol 287, R759-766.

Grabrucker, A.M., 2012. Environmental factors in autism. Front Psychiatry 3, 118.

Hamilton, N.B., Attwell, D., 2010. Do astrocytes really exocytose neurotransmitters? Nat Rev Neurosci 11, 227-238.

He, F., Sun, Y.E., 2007. Glial cells more than support cells? Int J Biochem Cell Biol 39, 661-665.

Horvath, S., Mirnics, K., 2013. Immune System Disturbances in Schizophrenia. Biol Psychiatry.

Ibi, D., Nagai, T., Kitahara, Y., Mizoguchi, H., Koike, H., Shiraki, A., Takuma, K., Kamei, H., Noda, Y., Nitta, A., Nabeshima, T., Yoneda, Y., Yamada, K., 2009. Neonatal polyI:C treatment in mice results in schizophrenia-like behavioral and neurochemical abnormalities in adulthood. Neurosci Res 64, 297-305.

Ibi, D., Nagai, T., Nakajima, A., Mizoguchi, H., Kawase, T., Tsuboi, D., Kano, S., Sato, Y., Hayakawa, M., Lange, U.C., Adams, D.J., Surani, M.A., Satoh, T., Sawa, A., Kaibuchi, K., Nabeshima, T., Yamada, K., 2013. Astroglial IFITM3 mediates neuronal impairments following neonatal immune challenge in mice. Glia 61, 679-693.

Ito, S., Kimura, K., Haneda, M., Ishida, Y., Sawada, M., Isobe, K., 2007. Induction of matrix metalloproteinases (MMP3, MMP12 and MMP13) expression in the microglia by amyloid-beta stimulation via the PI3K/Akt pathway. Exp Gerontol 42, 532-537.

Keene, S.D., Greco, T.M., Parastatidis, I., Lee, S.H., Hughes, E.G., Balice-Gordon, R.J., Speicher, D.W., Ischiropoulos, H., 2009. Mass spectrometric and computational analysis of cytokine-induced alterations in the astrocyte secretome. Proteomics 9, 768-782.

Khandaker, G.M., Zimbron, J., Dalman, C., Lewis, G., Jones, P.B., 2012. Childhood infection and adult schizophrenia: a meta-analysis of population-based studies. Schizophr Res 139, 161-168.

Kim, E.M., Shin, E.J., Choi, J.H., Son, H.J., Park, I.S., Joh, T.H., Hwang, O., 2010a. Matrix metalloproteinase-3 is increased and participates in neuronal apoptotic signaling downstream of caspase-12 during endoplasmic reticulum stress. J Biol Chem 285, 16444-16452.

Kim, S.T., Kim, E.M., Choi, J.H., Son, H.J., Ji, I.J., Joh, T.H., Chung, S.J., Hwang, O., 2010b. Matrix metalloproteinase-3 contributes to vulnerability of the nigral dopaminergic neurons. Neurochem Int 56, 161-167.

Kim, Y.S., Choi, D.H., Block, M.L., Lorenzl, S., Yang, L., Kim, Y.J., Sugama, S., Cho,

B.P., Hwang, O., Browne, S.E., Kim, S.Y., Hong, J.S., Beal, M.F., Joh, T.H., 2007. A pivotal role of matrix metalloproteinase-3 activity in dopaminergic neuronal degeneration via microglial activation. FASEB J 21, 179-187.

Kucukali, C.I., Aydin, M., Ozkok, E., Bilge, E., Orhan, N., Zengin, A., Kara, I., 2009. Do schizophrenia and bipolar disorders share a common disease susceptibility variant at the MMP3 gene? Prog Neuropsychopharmacol Biol Psychiatry 33, 557-561.

Lafon-Cazal, M., Adjali, O., Galeotti, N., Poncet, J., Jouin, P., Homburger, V., Bockaert, J., Marin, P., 2003. Proteomic analysis of astrocytic secretion in the mouse. Comparison with the cerebrospinal fluid proteome. J Biol Chem 278, 24438-24448.

Lai, W., Wu, J., Zou, X., Xie, J., Zhang, L., Zhao, X., Zhao, M., Wang, Q., Ji, J., 2013. Secretome analyses of Abeta(1-42) stimulated hippocampal astrocytes reveal that CXCL10 is involved in astrocyte migration. J Proteome Res 12, 832-843.

Levin, J., Giese, A., Boetzel, K., Israel, L., Hogen, T., Nubling, G., Kretzschmar, H., Lorenzl, S., 2009. Increased alpha-synuclein aggregation following limited cleavage by certain matrix metalloproteinases. Exp Neurol 215, 201-208.

Mercapide, J., Lopez De Cicco, R., Castresana, J.S., Klein-Szanto, A.J., 2003. Stromelysin-1/matrix metalloproteinase-3 (MMP-3) expression accounts for invasive properties of human astrocytoma cell lines. Int J Cancer 106, 676-682.

Meyer, U., Feldon, J., 2010. Epidemiology-driven neurodevelopmental animal models of schizophrenia. Prog Neurobiol 90, 285-326.

Meyer, U., Feldon, J., Schedlowski, M., Yee, B.K., 2005. Towards an immuno-precipitated neurodevelopmental animal model of schizophrenia. Neurosci Biobehav Rev 29, 913-947.

Moore, N.H., Costa, L.G., Shaffer, S.A., Goodlett, D.R., Guizzetti, M., 2009. Shotgun proteomics implicates extracellular matrix proteins and protease systems in neuronal

development induced by astrocyte cholinergic stimulation. J Neurochem 108, 891-908.

Nagai, T., Ibi, D., Yamada, K., 2011. Animal model for schizophrenia that reflects gene-environment interactions. Biol Pharm Bull 34, 1364-1368.

Nawa, H., Takei, N., 2006. Recent progress in animal modeling of immune inflammatory processes in schizophrenia: implication of specific cytokines. Neurosci Res 56, 2-13.

Noe, V., Fingleton, B., Jacobs, K., Crawford, H.C., Vermeulen, S., Steelant, W., Bruyneel, E., Matrisian, L.M., Mareel, M., 2001. Release of an invasion promoter E-cadherin fragment by matrilysin and stromelysin-1. J Cell Sci 114, 111-118.

O'Callaghan, E., Sham, P.C., Takei, N., Murray, G., Glover, G., Hare, E.H., Murray, R.M., 1994. The relationship of schizophrenic births to 16 infectious diseases. Br J Psychiatry 165, 353-356.

Olson, J.K., Miller, S.D., 2004. Microglia initiate central nervous system innate and adaptive immune responses through multiple TLRs. J Immunol 173, 3916-3924.

Ozawa, K., Hashimoto, K., Kishimoto, T., Shimizu, E., Ishikura, H., Iyo, M., 2006. Immune activation during pregnancy in mice leads to dopaminergic hyperfunction and cognitive impairment in the offspring: a neurodevelopmental animal model of schizophrenia. Biol Psychiatry 59, 546-554.

Pletnikov, M.V., Rubin, S.A., Vasudevan, K., Moran, T.H., Carbone, K.M., 1999. Developmental brain injury associated with abnormal play behavior in neonatally Borna disease virus-infected Lewis rats: a model of autism. Behav Brain Res 100, 43-50.

Revello, M.G., Gerna, G., 2004. Pathogenesis and prenatal diagnosis of human cytomegalovirus infection. J Clin Virol 29, 71-83.

Ripke, S., O'Dushlaine, C., Chambert, K., Moran, J.L., Kahler, A.K., Akterin, S.,

Bergen, S.E., Collins, A.L., Crowley, J.J., Fromer, M., Kim, Y., Lee, S.H., Magnusson, P.K., Sanchez, N., Stahl, E.A., Williams, S., Wray, N.R., Xia, K., Bettella, F., Borglum, A.D., Bulik-Sullivan, B.K., Cormican, P., Craddock, N., de Leeuw, C., Durmishi, N., Gill, M., Golimbet, V., Hamshere, M.L., Holmans, P., Hougaard, D.M., Kendler, K.S., Lin, K., Morris, D.W., Mors, O., Mortensen, P.B., Neale, B.M., O'Neill, F.A., Owen, M.J., Milovancevic, M.P., Posthuma, D., Powell, J., Richards, A.L., Riley, B.P., Ruderfer, D., Rujescu, D., Sigurdsson, E., Silagadze, T., Smit, A.B., Stefansson, H., Steinberg, S., Suvisaari, J., Tosato, S., Verhage, M., Walters, J.T., Multicenter Genetic Studies of Schizophrenia, C., Levinson, D.F., Gejman, P.V., Kendler, K.S., Laurent, C., Mowry, B.J., O'Donovan, M.C., Owen, M.J., Pulver, A.E., Riley, B.P., Schwab, S.G., Wildenauer, D.B., Dudbridge, F., Holmans, P., Shi, J., Albus, M., Alexander, M., Campion, D., Cohen, D., Dikeos, D., Duan, J., Eichhammer, P., Godard, S., Hansen, M., Lerer, F.B., Liang, K.Y., Maier, W., Mallet, J., Nertney, D.A., Nestadt, G., Norton, N., O'Neill, F.A., Papadimitriou, G.N., Ribble, R., Sanders, A.R., Silverman, J.M., Walsh, D., Williams, N.M., Wormley, B., Psychosis Endophenotypes International, C., Arranz, M.J., Bakker, S., Bender, S., Bramon, E., Collier, D., Crespo-Facorro, B., Hall, J., Iyegbe, C., Jablensky, A., Kahn, R.S., Kalaydjieva, L., Lawrie, S., Lewis, C.M., Lin, K., Linszen, D.H., Mata, I., McIntosh, A., Murray, R.M., Ophoff, R.A., Powell, J., Rujescu, D., Van Os, J., Walshe, M., Weisbrod, M., Wiersma, D., Wellcome Trust Case Control, C., Management, C., Donnelly, P., Barroso, I., Blackwell, J.M., Bramon, E., Brown, M.A., Casas, J.P., Corvin, A.P., Deloukas, P., Duncanson, A., Jankowski, J., Markus, H.S., Mathew, C.G., Palmer, C.N., Plomin, R., Rautanen, A., Sawcer, S.J., Trembath, R.C., Viswanathan, A.C., Wood, N.W., Data, Analysis, G., Spencer, C.C., Band, G., Bellenguez, C., Freeman, C., Hellenthal, G., Giannoulatou, E., Pirinen, M., Pearson, R.D., Strange, A., Su, Z., Vukcevic, D., Donnelly, P., Dna, G.D.Q.C., Informatics, G., Langford, C., Hunt, S.E., Edkins, S., Gwilliam, R., Blackburn, H., Bumpstead, S.J.,

Dronov, S., Gillman, M., Gray, E., Hammond, N., Jayakumar, A., McCann, O.T., Liddle, J., Potter, S.C., Ravindrarajah, R., Ricketts, M., Tashakkori-Ghanbaria, A., Waller, M.J., Weston, P., Widaa, S., Whittaker, P., Barroso, I., Deloukas, P., Publications, C., Mathew, C.G., Blackwell, J.M., Brown, M.A., Corvin, A.P., McCarthy, M.I., Spencer, C.C., Bramon, E., Corvin, A.P., O'Donovan, M.C., Stefansson, K., Scolnick, E., Purcell, S., McCarroll, S.A., Sklar, P., Hultman, C.M., Sullivan, P.F., 2013. Genome-wide association analysis identifies 13 new risk loci for schizophrenia. Nat Genet 45, 1150-1159.

Rubin, S.A., Sylves, P., Vogel, M., Pletnikov, M., Moran, T.H., Schwartz, G.J., Carbone, K.M., 1999. Borna disease virus-induced hippocampal dentate gyrus damage is associated with spatial learning and memory deficits. Brain Res Bull 48, 23-30.

Schmidt-Kastner, R., van Os, J., Esquivel, G., Steinbusch, H.W., Rutten, B.P., 2012. An environmental analysis of genes associated with schizophrenia: hypoxia and vascular factors as interacting elements in the neurodevelopmental model. Mol Psychiatry 17, 1194-1205.

Schulze-Tanzil, G., de Souza, P., Merker, H.J., Shakibaei, M., 2001. Co-localization of integrins and matrix metalloproteinases in the extracellular matrix of chondrocyte cultures. Histol Histopathol 16, 1081-1089.

Shi, L., Fatemi, S.H., Sidwell, R.W., Patterson, P.H., 2003. Maternal influenza infection causes marked behavioral and pharmacological changes in the offspring. J Neurosci 23, 297-302.

Skorupa, A., Urbach, S., Vigy, O., King, M.A., Chaumont-Dubel, S., Prehn, J.H., Marin, P., 2013. Angiogenin induces modifications in the astrocyte secretome: Relevance to amyotrophic lateral sclerosis. J Proteomics 91C, 274-285.

Smith, S.E., Li, J., Garbett, K., Mirnics, K., Patterson, P.H., 2007. Maternal immune activation alters fetal brain development through interleukin-6. J Neurosci 27,

10695-10702.

Takeuchi, O., Akira, S., 2007. Recognition of viruses by innate immunity. Immunol Rev 220, 214-224.

Town, T., Jeng, D., Alexopoulou, L., Tan, J., Flavell, R.A., 2006. Microglia recognize double-stranded RNA via TLR3. J Immunol 176, 3804-3812.

Ullian, E.M., Christopherson, K.S., Barres, B.A., 2004. Role for glia in synaptogenesis. Glia 47, 209-216.

van Dongen, J., Boomsma, D.I., 2013. The evolutionary paradox and the missing heritability of schizophrenia. Am J Med Genet B Neuropsychiatr Genet 162B, 122-136.

Volterra, A., Meldolesi, J., 2005. Astrocytes, from brain glue to communication elements: the revolution continues. Nat Rev Neurosci 6, 626-640.

Walters, J.T., Rujescu, D., Franke, B., Giegling, I., Vasquez, A.A., Hargreaves, A., Russo, G., Morris, D.W., Hoogman, M., Da Costa, A., Moskvina, V., Fernandez, G., Gill, M., Corvin, A., O'Donovan, M.C., Donohoe, G., Owen, M.J., 2013. The role of the major histocompatibility complex region in cognition and brain structure: a schizophrenia GWAS follow-up. Am J Psychiatry 170, 877-885.

Wang, D.D., Bordey, A., 2008. The astrocyte odyssey. Prog Neurobiol 86, 342-367.

Witek-Zawada, B., Koj, A., 2003. Regulation of expression of stromyelysin-1 by proinflammatory cytokines in mouse brain astrocytes. J Physiol Pharmacol 54, 489-496.

Yan, E., Castillo-Melendez, M., Nicholls, T., Hirst, J., Walker, D., 2004. Cerebrovascular responses in the fetal sheep brain to low-dose endotoxin. Pediatr Res 55, 855-863.

Ye, S., Eriksson, P., Hamsten, A., Kurkinen, M., Humphries, S.E., Henney, A.M., 1996. Progression of coronary atherosclerosis is associated with a common genetic variant

of the human stromelysin-1 promoter which results in reduced gene expression. J Biol Chem 271, 13055-13060.

Figure Legends

Fig. 1. 2D-DIGE analysis in polyI:C-ACM

(A) A representative 2D-DIGE image of CyDye-labeled proteins derived from polyI:C-ACM (red) and control-ACM (green). Astrocytes were prepared from cortices and hippocampi of neonatal ICR mice and ACM were obtained 24 h after drug treatment. ACM: astrocyte-conditioned medium. (B) Boxes I to X show areas with differentially expressed protein spots that were excised and identified by LC-MS/MS. Arrows indicate identified protein spots with their spot numbers (see Table 1).

Fig. 2. Expression level of Mmp3 in polyI:C-ACM and astrocytes

(A) Representative western blot images of Mmp3 protein expression in ACM and astrocyte cell lysates at 6 h, 12 h and 24 h after polyI:C treatment. (B) Mmp3 mRNA level in polyI:C-treated astrocytes at 6 h, 12 h and 24 h after polyI:C treatment. Values indicate the means ± SE (n = 3). **p<0.01 versus control treatment. (C, D) Mmp3 protein level in polyI:C-treated astrocytes (C) and polyI:C-ACM (D) at 6 h, 12 h and 24 h after treatment. Values indicate the means ± SE (n = 9 for astrocytes, n = 6 for ACM). **p<0.01 versus control treatment and control-ACM, respectively. (E) Caseinolytic activity of Mmp3 in polyI:C-ACM. Values are the means ± SE (n = 4). *p<0.05 versus control-ACM.

Fig. 3. Changes in the Mmp3 and Tlr3 expression in polyI:C-treated astrocyte and microglia

(A) Tlr3 mRNA level in polyI:C-treated astrocyte and microglia. Values indicate the means ± SE (n = 4). **p<0.01 versus control. N.S.: not significant. (B) Mmp3 mRNA level in polyI:C-treated astrocyte and microglia. Values indicate

the means ± SE (n = 6 for astrocytes, n = 7 for microglia). **p<0.01 versus control. (C) Mmp3 protein level in polyI:C-ACM and polyI:C-MCM. Values indicate the means ± SE (n = 4). **p<0.01 versus control. CM: conditioned medium. N.D., not detectable.

Fig. 4. Effect of Mmp3 on dendritic elongation of primary cultured neurons

(A) Representative images of MAP2-positive dendrites of primary cultured neurons (DIV7). Neurons were cultured for 5 days (DIV2-7) with control-ACM supplemented with the indicated concentration of rmMmp3 or vehicle. (B) MAP2-positive dendrite length of neurons cultured with control-ACM supplemented with the indicated doses of rmMmp3 or vehicle (DIV7). Values indicate the means ± SE of three independent experiments (n = 36-38). **p<0.01 versus vehicle-treated control-ACM. Scale bar, 50 μm.

Fig. 5. Effect of Mmp3 knockdown in astrocytes on polyI:C-ACM-induced impairments of neuronal development

Astrocytes were transfected with control siRNA (CON), Mmp3 siRNA #1 (#1) or Mmp3 siRNA #2 (#2) before polyI:C or vehicle treatment and then ACM and cell lysate samples were prepared 24 h after polyI:C treatment. (A) Representative western blot images of Mmp3 protein level in ACM and cell lysates derived from siRNA-treated astrocytes. (B) Mmp3 mRNA level in cell lysates derived from siRNA-treated astrocytes. Values indicate the means ± SE (n = 4). **p<0.01 versus control siRNA and vehicle-treated cell lysate, ##p<0.01 versus control siRNA and polyI:C-treated cell lysate. (C) Mmp3 protein level in cell lysates derived from siRNA-treated astrocytes. Values indicate the means ± SE (n = 4). *p<0.05 versus control siRNA and vehicle-treated cell lysate, #p<0.05 versus control siRNA and

polyI:C-treated cell lysate. (D) Mmp3 protein level in ACM derived from siRNA-treated astrocytes. Values indicate the means ± SE (n = 4). **p<0.01 versus control-ACM, ##p<0.01 versus control siRNA-treated polyI:C-ACM. (E) Effect of polyI:C-ACM derived from Mmp3 knockdown astrocytes on MAP2-positive dendrite length of primary cultured neurons (DIV7). Neurons were cultured for 5 days (DIV2-7) with control-ACM or polyI:C-ACM derived from astrocytes transfected with control siRNA (CON) or Mmp3 siRNA (#1 or #2). Values indicate the means ± SE of more than three independent experiments (n = 28-59). **p<0.01 versus control-ACM, ##p<0.01 versus control siRNA-treated polyI:C-ACM. Scale bar, 50 μm.

Table(s)

Table 1. Results of 2D-DIGE analysis of CyDye-labeled proteins derived from polyI:C-ACM and control-ACM.

Spot No.[a]	Control-ACM[b]			PolyIC-ACM[b]			Fold change[c]	P-value[d]
1	11.9	±	8.0	247.6	±	88.4	20.81	0.029
2	155.1	±	43.7	47.5	±	10.9	0.31	0.044
3	910.8	±	85.4	571.5	±	70.2	0.63	0.015
4	731.6	±	109.7	349.4	±	84.6	0.48	0.025
5	495.4	±	108.0	223.8	±	44.0	0.45	0.048
6	216.8	±	23.8	108.7	±	21.5	0.50	0.010
7	21116.8	±	1413.6	38788.8	±	6376.1	1.84	0.027
8	161.0	±	18.0	104.2	±	14.2	0.65	0.038
9	2051.9	±	212.3	1365.2	±	187.4	0.67	0.042
10	296.4	±	116.2	27.4	±	9.4	0.09	0.050
11	2208.0	±	238.5	1083.3	±	306.1	0.49	0.020
12	799.3	±	143.2	428.5	±	50.7	0.54	0.041
13	2521.6	±	379.8	1079.1	±	406.4	0.43	0.032

[a]Differentially expressed protein spots in ACM were determined by the PDQuest software (See fig. 1).

[b]Values indicate spot intensity of each protein spot calculated in the PDQuest software (means±SE, n = 5).

[c]Fold change is calculated as the ratio of the average intensity of each spot in polyI:C-ACM to control-ACM.

[d]Student's t-test was applied to determine the differentially expressed spots between polyI:C-ACM and control-ACM.

Table(s)

Table 2. Protein identification of differentially expressed spots in polyI:C-ACM.

Spot No.	Experimental[a]		Theoretical		Peptides identified	Coverage (%)	MASCOT score	Protein name	Gene symbol
	MW (kDa)	pI	MW (kDa)	pI					
1	46	4.45	35	5.68	7	23	274	Follistatin-related protein 1	Fstl1
2	16	5.10	16	5.28	7	35	157	Coactosin-like protein	Cotl1
			15	5.32	2	14	68	Galectin-1	Lgals1
			17	5.08	1	8	60	Eukaryotic translation initiation factor 5A-1	Eif5a
			17	5.08	1	16	53	Glia maturation factor beta	Gmfb
3	49	5.19	46	6.48	10	24	381	Pigment epithelium-derived factor	Serpinf1
			48	5.00	4	12	259	Protein disulfide-isomerase A6	Pdia6
4	44	5.40	37	5.57	8	23	315	Cathepsin B	Ctsb
5	42	5.55	43	5.53	3	10	142	Serpin B6	Serpinb6
6	45	5.54	43	5.40	15	33	455	Creatine kinase B-type	Ckb
7	60	5.50	54	5.74	29	40	1015	Stromelysin-1	Mmp3
8	34	5.65	37	5.70	7	23	391	L-lactate dehydrogenase B chain	Ldhb
9	47	6.02	47	6.37	5	16	301	Alpha-enolase	Eno1
10	22	6.40	26	6.77	5	17	124	Glutathione S-transferase A4	Gsta4
			24	7.68	2	10	97	Glutathione S-transferase P 1	Gstp1
11	47	6.10	45	6.71	25	38	530	Cathepsin D	Ctsd
12	25	7.30	26	7.71	18	58	529	Glutathione S-transferase Mu 1	Gstm1
13	67	6.68	61	8.29	28	35	767	Beta-hexosaminidase subunit beta	Hexb

[a]Experimental molecular weight (MW) and isoelectric point (pI) were determined by the location of each spot in a preparative gel.

Figure(s)

Fig. 1. (Yamada et al.)

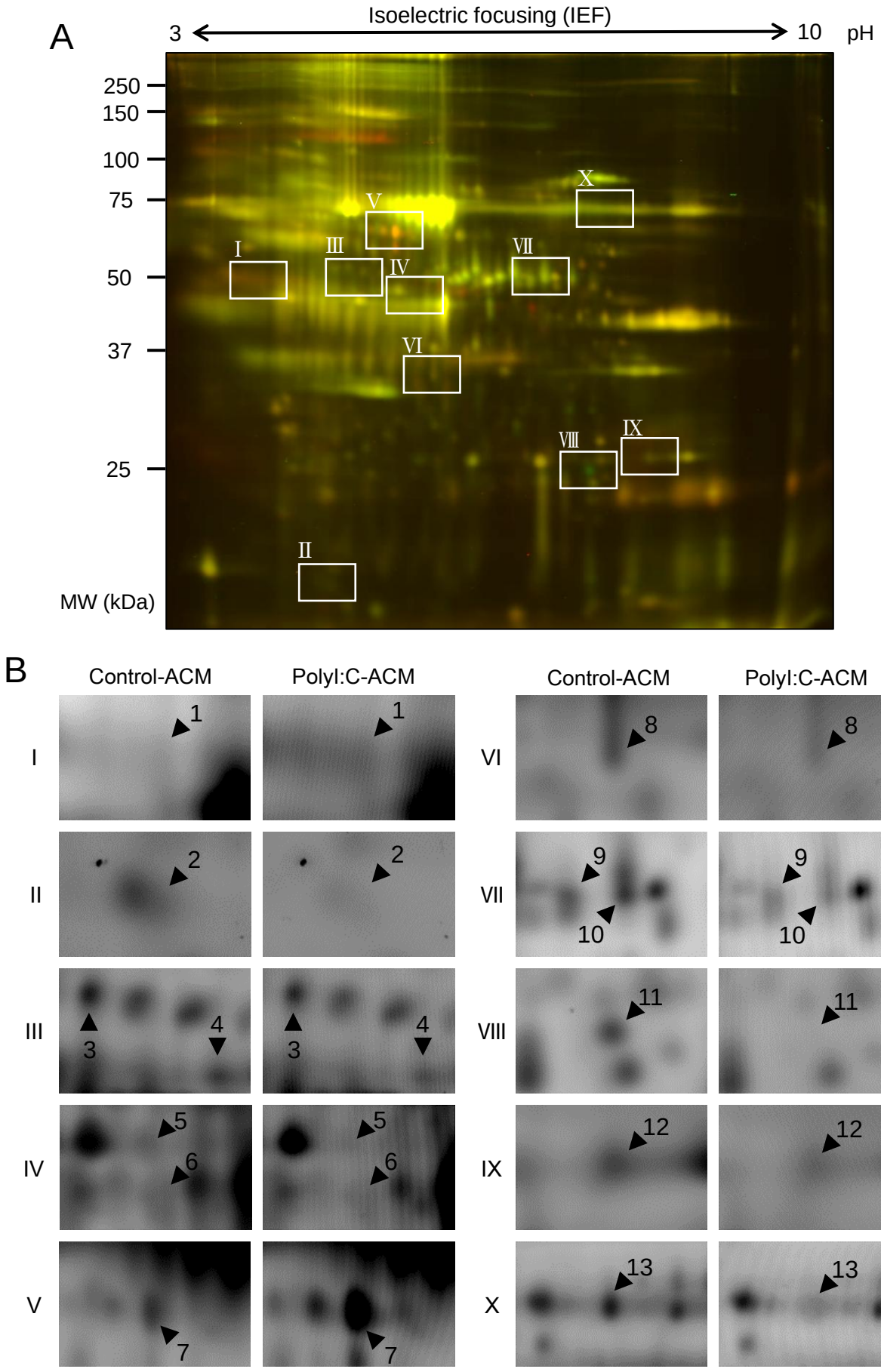

Fig. 2. (Yamada et al.)

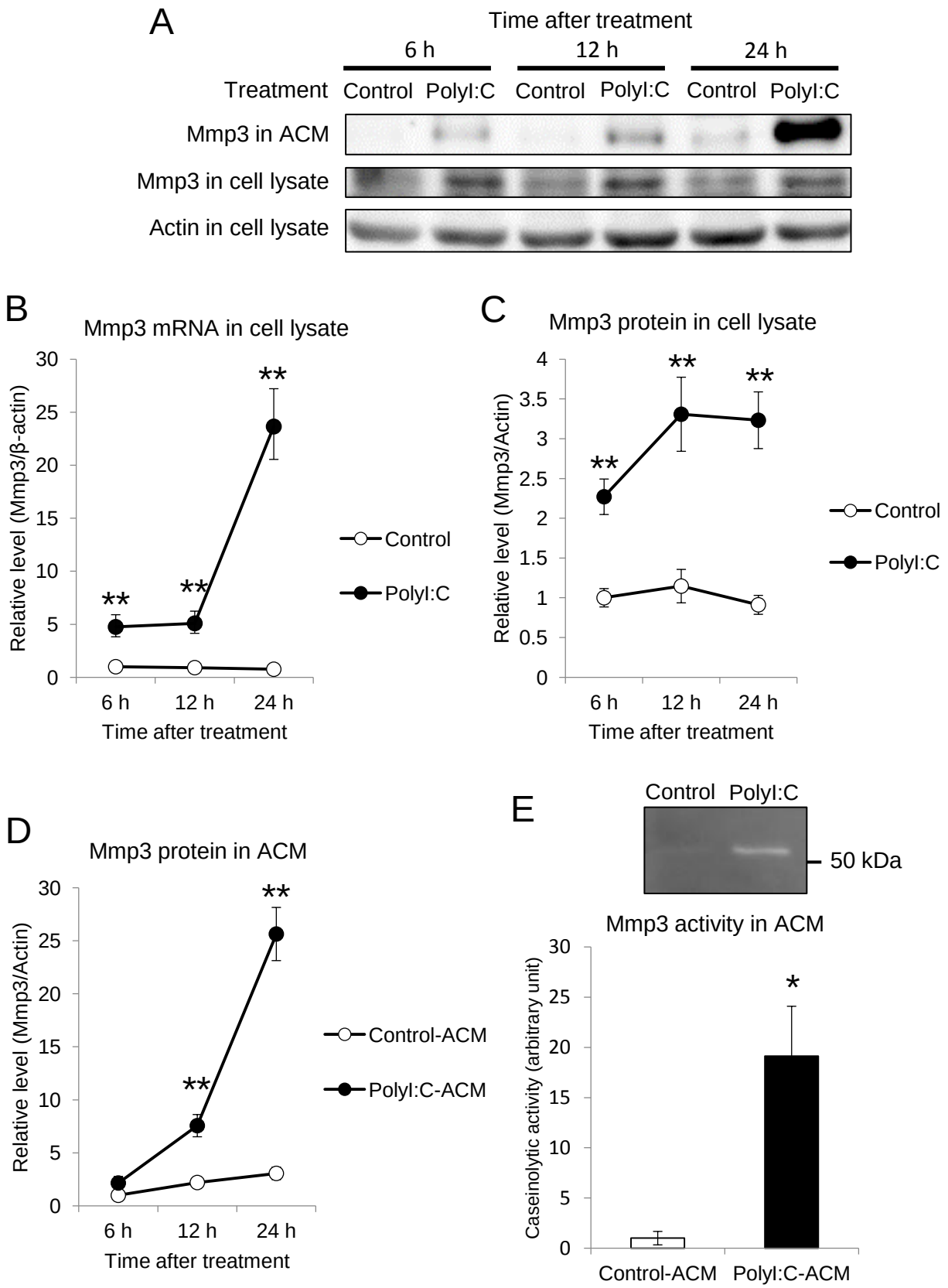

Fig. 3. (Yamada et al.)

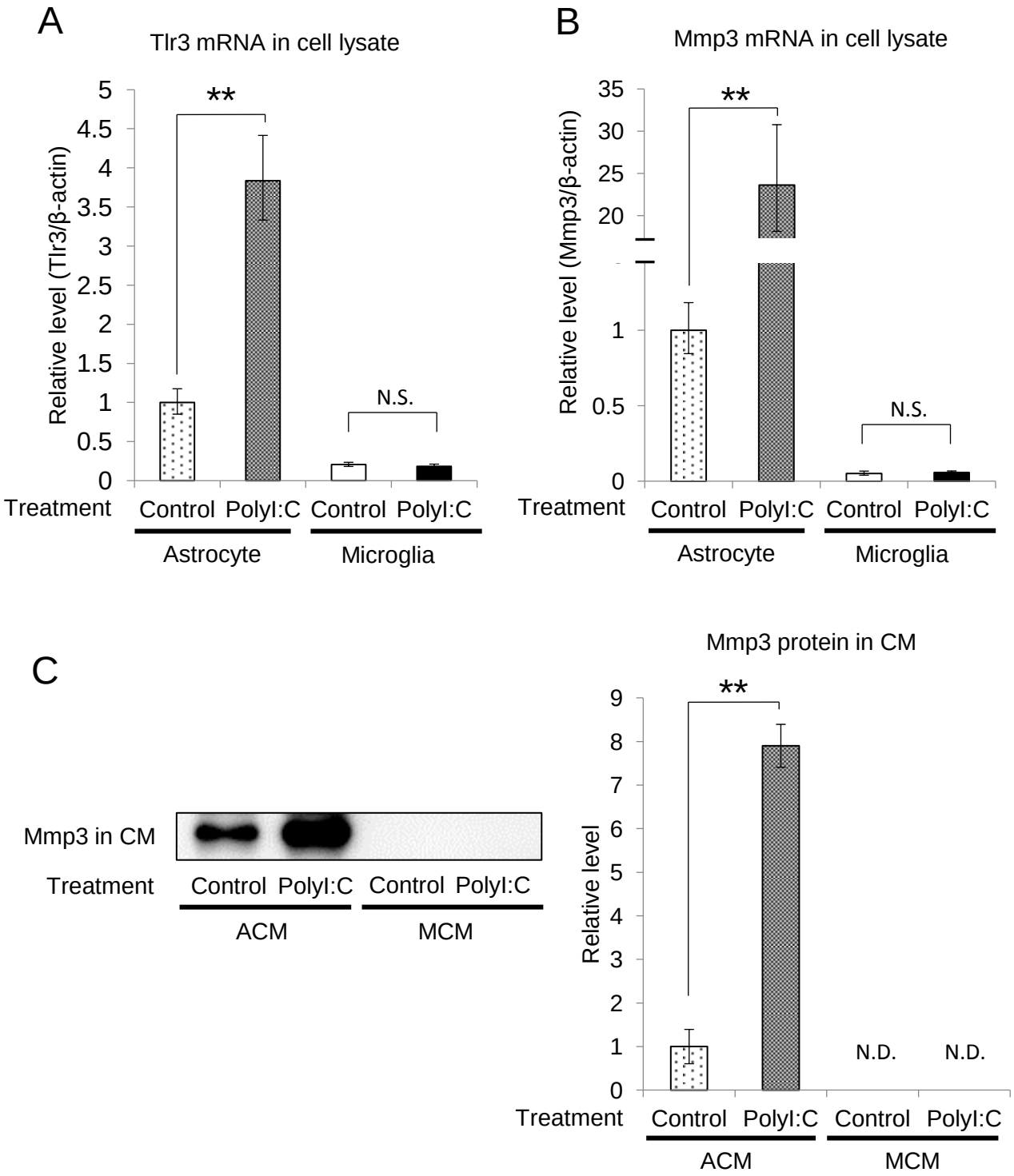

Fig. 4. (Yamada et al.)

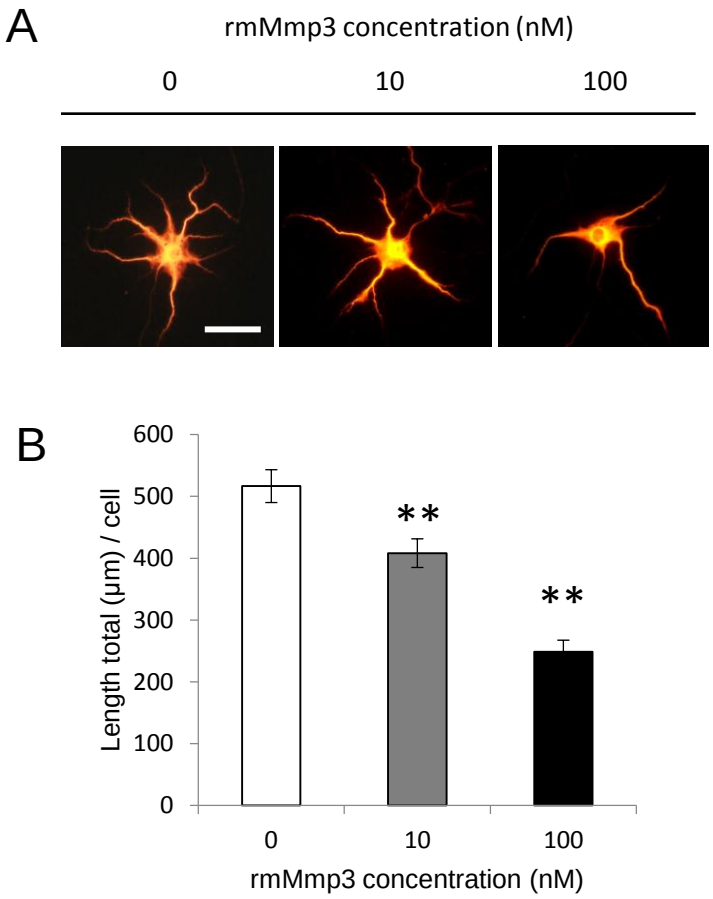

Fig. 5. (Yamada et al.)